On the banded microstructures in CoCrMo-Ni in-situ alloyed through laser powder bed fusion

Siyuan Wei[1,*], Yakai Zhao[1], Baicheng Zhang[2], Pei Wang[1,*], Upadrasta Ramamurty[1,3]

[1]*Institute of Materials Research and Engineering, Agency for Science, Technology and Research, Singapore 138634, Republic of Singapore.*

[2]*Advanced Material & Technology Institute, University of Science and Technology Beijing, Beijing 100083, P.R. China.*

[3]*School of Mechanical and Aerospace Engineering, Nanyang Technological University, Singapore 639798, Republic of Singapore.*

*Corresponding authors: wei_siyuan@imre.a-star.edu.sg; wangp@imre.a-star.edu.sg

Abstract:

Heterogenous banded microstructure was observed throughout a compositionally graded CoCrMo-Ni alloy using mixed CoCrMo and Ni powders and the laser powder bed fusion (LPBF) technique. Such a banded structure is a result of the melt pools having large width-to-depth aspect ratio, which favors grain growth towards its center. A continuous alignment of the growing grains towards the temperature gradient makes them appear to be 'chasing' the trailing edge of the melt pool. Therefore, the observed grain morphology varies with the viewing direction, which, in combination with the scan rotation of 67°, results in the appearance of an alternating grain morphology along the build direction. These findings bring attention to the new possibility of tailoring heterogeneous grain structures that can enhance the mechanical properties of the AM parts. This approach can be readily applied to other types of alloys, thereby enriching the alloy design tools available for microstructural engineering.

Keywords: laser powder bed fusion; grains; heterogeneity.

1. Introduction

A unique advantage of additive manufacturing (AM) of alloys is that it allows for the near-net fabrication of engineering parts with complex geometries[1]. Because of this, however, manipulation of the microstructures through thermo-mechanical processing—a common technique to impart the desired mechanical performance to the alloy—is not viable. In its absence, the micro- and meso-structures in AM alloys using techniques such as laser powder bed fusion (LPBF) can be modulated by manipulating the fabrication parameters and/or compositions[2-4]. For example, a columnar to equiaxed grain structure transition in Ti-6Al-4V can be imparted by altering the scan rotation from 90° to 67°[2]. Since such tailored microstructures can significantly enhance the performance of the AM alloys, more research efforts are being directed at the microstructural engineering of AM alloys.

One promising approach is the creation of *heterogeneities*, which could enhance the overall mechanical performance of the AM alloy through interaction between chemical and/or microstructural heterogeneities, as known as kinematic (or back-stress) hardening[1,3]. In this context, we recently investigated the chemical heterogeneities in compositionally graded CoCrMo-Ni alloys and found that they play a significant role in the local and overall mechanical properties [5]. In the present work, we further report the microstructural heterogeneities within the graded alloy, *i.e.,* two types of mesostructural bands with distinct grain morphologies. Through the elucidation of underlying reasons for the banded microstructure observed along the build direction (BD), we believe that the mechanism uncovered here can utilized for understanding the microstructural development in other alloy systems fabricated using LPBF and other AM techniques. Such an understanding, in turn, has the potential to enrich the design tools available for engineering microstructural heterogeneities.

2. Methods

The compositionally graded CoCrMo-Ni alloy was fabricated using an in-house developed LPBF setup[5], which allows for processing of graded coupons with pre-determined compositional gradations using mixed powders of two different feedstocks. The compositions vary from $(CoCrMo)_{1.2}Ni_{98.8}$ to $(CoCrMo)_{73.2}Ni_{26.8}$ (in at.%, and all the compositions are presented in at.% hereafter). Its processing is briefly described below (while details can be found in our previous work[5]). Pre-alloyed $Co_{65}Cr_{29}Mo_6$ and elemental Ni powders, both having spherical shape (from gas atomization) and diameters ranging ~15–53 μm, were used as feedstock. A block of graded alloy with minimum porosity (120, 60, and 10 in length, width,

and height, respectively) was fabricated using bi-directional scanning with 67° rotation, laser spot size 35 μm, laser power 305 W, scan speed 960 mm/s, hatch spacing 90 μm, and layer thickness 40 μm. Scanning electron microscopy (SEM) equipped with energy-dispersive X-ray spectroscopy (EDS), electron backscatter diffraction (EBSD), and backscattered electron (BSE) detectors were used for the microstructural characterizations on the mechanically mirror polished samples. Vickers hardness testing was performed on the top surface of the graded samples with 500 g force and 10 s hold time.

3. Results and discussion

The achieved compositional gradient is illustrated in Figure 1, using Ni as an indicator. The Ni content varies in 26.8–98.8 at.%, which leads to an overall composition range from $(CoCrMo)_{1.2}Ni_{98.8}$ to $(CoCrMo)_{73.2}Ni_{26.8}$. Despite such a large compositional variation, the whole block of graded sample shows single-phase face-centered cubic (FCC) structure (examined using EBSD, and the examples are shown in Figure S1 in the supplementary information). The Vickers hardness across the graded sample was also plotted in Figure 1. Obviously, decreasing Ni content leads to increasing hardness, and the peak hardness occurs at $(CoCrMo)_{68.5}Ni_{31.5}$. Detailed characterization on the mechanical behavior can be found in our previous work[5].

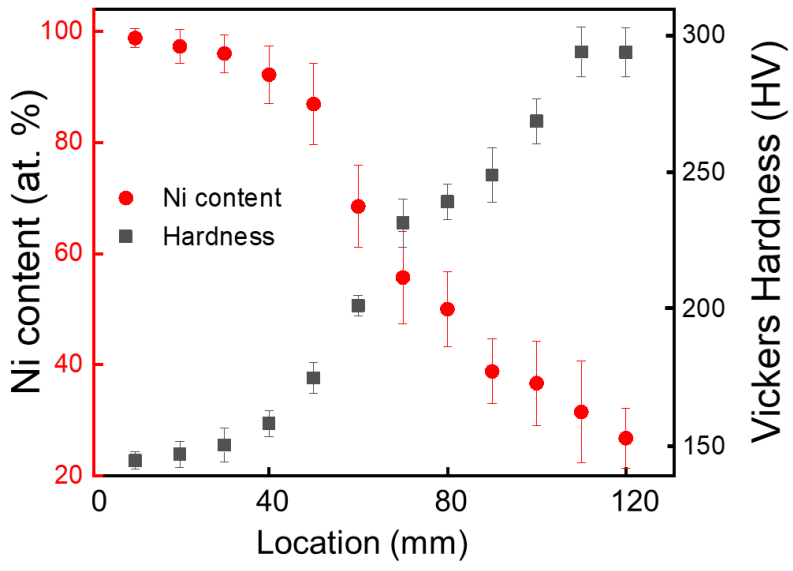

Figure 1. Average Ni content and Vickers hardness at varying locations in the compositionally graded alloy.

Microstructural characterization revealed two distinct types of grains (denoted as Types I and II hereafter) that form alternating bands in each of the sectioned sample. Representative

BSE images of $(CoCrMo)_{68.5}Ni_{31.5}$ and $(CoCrMo)_{2.7}Ni_{97.3}$ are shown in Figure 2(a), and 2(b), respectively. Type I grains, highlighted with blue rectangles, have well-defined melt-pool shaped boundaries with fine grains growing laterally, as schematically illustrated in Figures 2(c). Type II grains highlighted with orange rectangles and illustrated in Figures 2(d), on the contrary, tend to grow towards the center of the melt pool. Note that the melt-pool-shaped structures are a result of cyclic heating/cooling, not the morphology of a single melt pool.

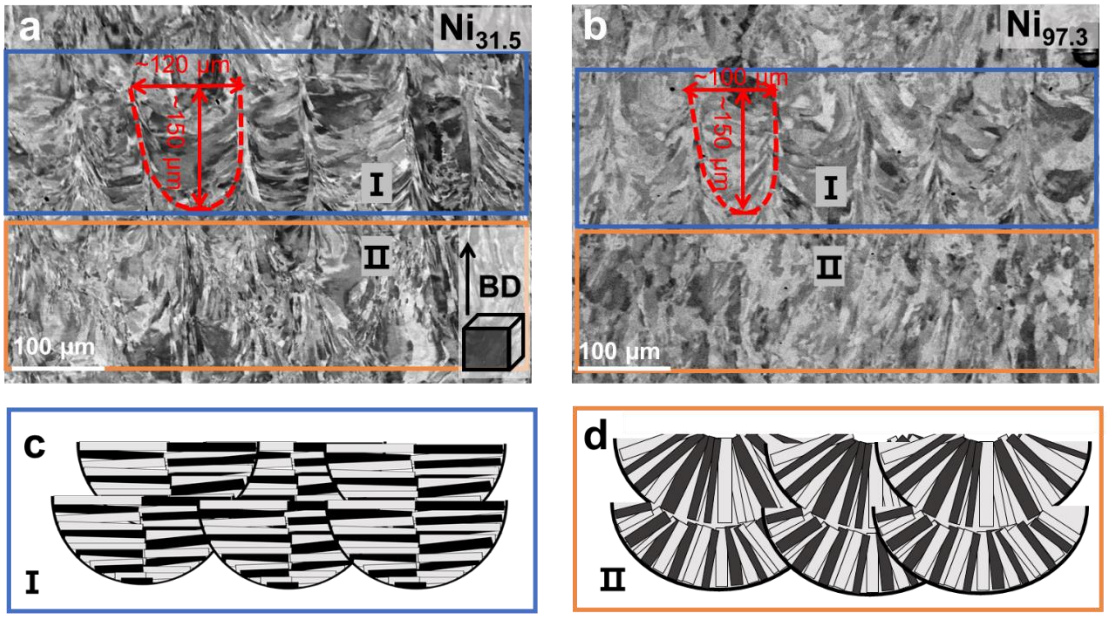

Figure 2. Representative BSE micrographs of Type I and II grains observed in (a) $(CoCrMo)_{68.5}Ni_{31.5}$ and (b) $(CoCrMo)_{2.7}Ni_{97.3}$ samples. Blue and orange rectangles highlight different grain morphologies, which are schematically illustrated in (c) and (d), respectively.

Columnar grains are generally favored in LPBF process (when other grain refinement mechanisms, e.g., inoculating nanoparticles as grain nucleation sites[6], are absent), and their growth typically initiates from the melt pool boundaries and proceeds along the maximum heat flow direction, normal to the solidifying surface of the melt pool[7]. Therefore, melt pools with high aspect ratio would favor grain growth towards the center of the melt pool, whereas those with low aspect ratio can result in grains that are aligned along the BD. Moreover, the local growth direction of grains can be affected by the moving melt pool during printing, induced by the 3-dimensional (3D) local curvature of the solidification interface[7]. Under such scenario, the columnar grains would continuously align their growth towards the temperature gradient, eventually appearing to be 'chasing' the trailing edge of the scan track[7,8], as schematically illustrated in Figure 3. As a result, the observed grain morphology would vary according to the viewing angle.

Based on this, the formation mechanisms of the alternating Type I and II grains can be described as follows. Type I grains are observed when the viewing direction is parallel to the scan direction (*x* axis in Figure 3(a)). Type II grains are observed when the viewing direction is perpendicular to the scan direction (*y* axis in Figure 3(b)). Therefore, the observed grain morphologies in 2D would appear disparate depending on the angle between the scan direction (marked by the arrows in each layer) and viewing direction, θ, in Figure 3(c), although the microstructure remains the same in 3D.

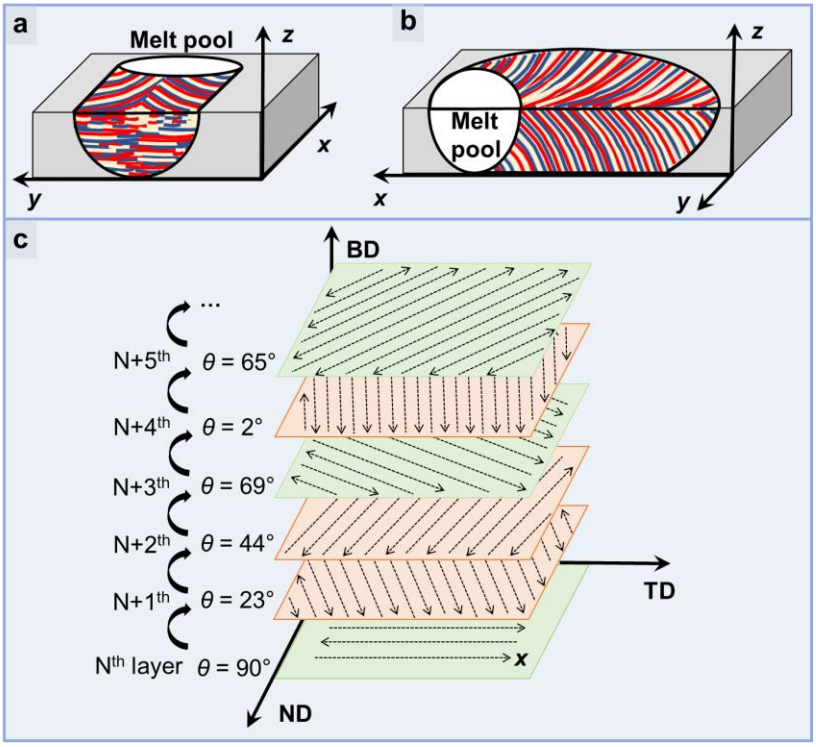

Figure 3. Schematic illustrations of the relationship between a moving melt pool and grains that are 'tailing' it, which are viewed (a) parallel and (b) perpendicular to scan direction (*x* axis). (c) Schematic of the effect of 67° scan rotations, where arrows indicate the scan directions (*x* axis in (a) and (b)). Green and orange colors were utilized to represent the varying grain structures.

To examine the effect of melt pool shape on the grain morphologies, an additional $(CoCrMo)_{68.5}Ni_{31.5}$ sample was fabricated using the same set of Ni and $Co_{65}Cr_{29}Mo_6$ feedstock powders. Except for changing the laser spot size from ~35 to ~80 μm, other fabrication parameters were kept the same. The melt pool shapes at the top layers of both samples were characterized by BSE imaging (Figure 4). It is evident that the melt pools in sample A (extracted from graded alloy coupon) exhibit a higher aspect ratio than those in sample B (fabricated additionally). The differences in the melt pool shapes can be attributed to the size of the laser spot size utilized. A larger laser spot size leads to lower volumetric energy density,

which, in turn, results in a melt pool of smaller aspect ratio[9]. Consequently, when grains grow along the maximum heat flow direction, which is typically normal to the melt pool boundary[7], columnar grains aligned along the BD are observed in samples fabricated with melt pools with smaller aspect ratio (sample B). Crystallographic orientation maps on multiple layers (500×500 μm^2 scanning area), show distinct grain morphologies and textures in the two samples. Instead of the banded Type I and II grains, columnar grains with strong <001>-oriented texture prevail in sample B. Above results further confirm that the melt pool shape is one of the key aspects affecting the grain morphology.

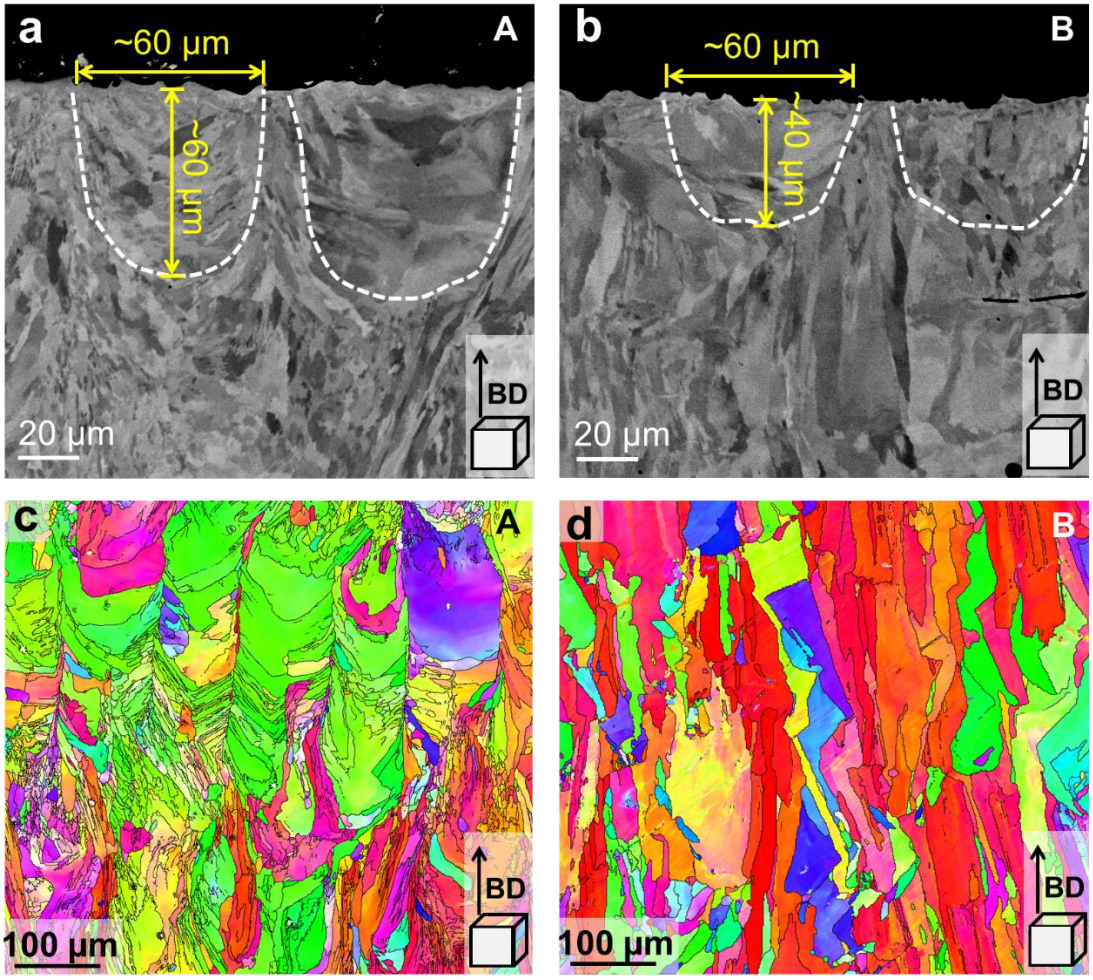

Figure 4. BSE images of the top layers of the two $Co_{43.6}Cr_{22.3}Mo_{2.6}Ni_{31.5}$ samples: (a) from the graded coupon, named as sample A, (b) same composition fabricated additionally, denoted as sample B. (c–d) EBSD maps of samples A and B, respectively.

4. Summary

A compositionally graded CoCrMo-Ni alloy was fabricated using an in-house developed LPBF setup, with compositions varying from $(CoCrMo)_{1.2}Ni_{98.8}$ to $(CoCrMo)_{73.2}Ni_{26.8}$. Microstructural investigations revealed the following key findings:

1) A banded microstructure with two distinct grain morphologies was found throughout the graded alloys despite the large compositional variations.
2) The following two key factors are the reasons behind the formation of the banded grain structure: (i) melt pool with relatively large aspect ratio, and (ii) varying angles between the viewing and the laser scanning directions.

In the broader context of the other alloys produced using LPBF (and other AM techniques), this work highlights a new possibility of tailoring microstructural heterogeneities to enhance their mechanical properties.

Declaration of competing interest

The authors declare that they have no known competing financial interests or personal relationships that could have appeared to influence the work reported in this paper.

Acknowledgement

This work was supported by Agency for Science, Technology and Research (A*STAR) of Singapore via the Structural Metal Alloys Programme (No. A18B1b0061) and Development of High-Performance Electric Traction Module (No. M22K4a0044).

Reference

[1] S. Wei, C. Hutchinson, U. Ramamurty, Mesostructure engineering in additive manufacturing of alloys, Scripta Materialia 230 (2023) 115429.
[2] P. Kumar, O. Prakash, U. Ramamurty, Micro-and meso-structures and their influence on mechanical properties of selectively laser melted Ti-6Al-4V, Acta Materialia 154 (2018) 246-260.
[3] E. Alabort, Y. T. Tang, D. Barba, R. C. Reed, Alloys-by-design: A low-modulus titanium alloy for additively manufactured biomedical implants, Acta Materialia 229 (2022) 117749.
[4] A. Zafari, K. Xia, Superior titanium from hybridised microstructures – A new strategy for future alloys, Scripta Materialia 173 (2019) 61-65.
[5] S. Wei, Y. Zhao, B. Zhang, P. Wang, U. Ramamurty, Mesoscopic chemical heterogeneities in laser powder bed fused CoCrMo and Ni mixed powders and their effect on the mechanical properties, Materials Science and Engineering: A 888 (2023) 145795.
[6] J. H. Martin, B. D. Yahata, J. M. Hundley, J. A. Mayer, T. A. Schaedler, T. M. Pollock, 3D printing of high-strength aluminium alloys, Nature 549 (2017) 365-369.
[7] H. L. Wei, J. W. Elmer, T. DebRoy, Origin of grain orientation during solidification of an aluminum alloy, Acta Materialia 115 (2016) 123-131.
[8] S. David, J. Vitek, Correlation between solidification parameters and weld microstructures, International Materials Reviews 34 (1989) 213-245.
[9] J. S. Weaver, J. C. Heigel, B. M. Lane, Laser spot size and scaling laws for laser beam additive manufacturing, J Mater Process Technol 73 (2022).